

Dynamic Relevance Learning for Few-Shot Object Detection

Weijie Liu, Chong Wang*, *Member, IEEE*, Haohe Li, Shenghao Yu, Song Chen, Xulun Ye and Jiafei Wu

Abstract—Expensive bounding-box annotations have limited the development of object detection task. Thus, it is necessary to focus on more challenging task of few-shot object detection. It requires the detector to recognize objects of novel classes with only a few training samples. Nowadays, many existing popular methods based on meta-learning have achieved promising performance, such as Meta R-CNN series. However, only a single category of support data is used as the attention to guide the detecting of query images each time. Their relevance to each other remains unexploited. Moreover, a lot of recent works treat the support data and query images as independent branch without considering the relationship between them. To address this issue, we propose a dynamic relevance learning model, which utilizes the relationship between all support images and Region of Interest (RoI) on the query images to construct a dynamic graph convolutional network (GCN). By adjusting the prediction distribution of the base detector using the output of this GCN, the proposed model can guide the detector to improve the class representation implicitly. Comprehensive experiments have been conducted on Pascal VOC and MS-COCO dataset. The proposed model achieves the best overall performance, which shows its effectiveness of learning more generalized features. Our code is available at <https://github.com/liuweijie19980216/DRL-for-FSOD>.

Index Terms—Few-Shot Object Detection, Meta R-CNN, Graph Convolutional Networks, Dynamic Relevance Learning

I. INTRODUCTION

With the rapid development of deep learning, computers have surpassed human beings in an increasing number of aspects, such as image classification [1]. However, as far as current technologies are concerned, a large amount of labeled data must be provided so that machines can learn to adapt new tasks. In contrast, human can recognize a certain animal just by looking at a picture once. In order to further narrow the gap between the computer and human, how to make model learn a new task through only limited labeled samples has gradually become a hot research topic.

The few-shot learning is regarded as one of the applications of meta-learning in supervised learning. Meta-learning aims to

Manuscript received July 26, 2021. This work was supported in part by the Zhejiang Provincial Natural Science Foundation of China (No. LY20F030005) and in part by the National Natural Science Foundation of China (No. 61603202). (Corresponding author: Chong Wang.)

W. Liu, C. Wang, H. Li, S. Yu, S. Chen and X. Ye are with the Faculty of Electrical Engineering and Computer Science, Ningbo University, China (e-mail: liuweijie19980216@gmail.com; wangchong@nbu.edu.cn; lihaohe1023@163.com; ysh_nbu@163.com; 1195780343@qq.com; yexulun@nbu.edu.cn).

J. Wu is with SenseTime Research, China (e-mail: wujiafei@sensetime.com).

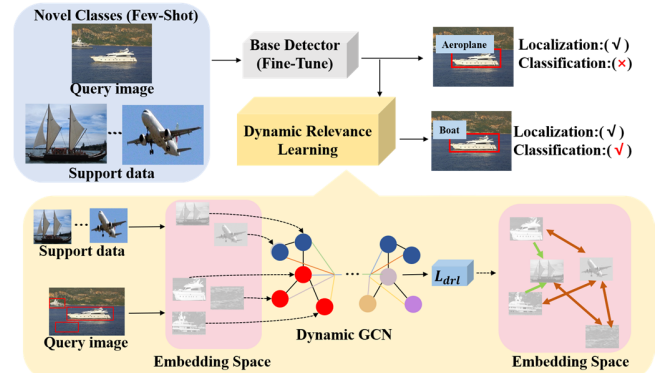


Fig. 1. Illustration of dynamic relevance learning. The classification loss is calculated by RoI embeddings output from GCN, which can make RoI features close to support features of the same category.

design a universal strategy to capture structural changes between different tasks by accumulating knowledge. In this way, when the model encounters a new task, it can quickly learn to handle it. In other words, it makes the model learn to learn. Normally, meta-learning is based on four kinds of techniques, namely data augmentation [2, 3, 4], external memory [5, 6], parameter optimization [7, 8] and metric learning [9, 10, 11].

At present, the few-shot learning has been widely used in computer vision, such as image and video classification [2, 4, 7-14], generation [3, 15], translation [16], object detection [17-20] and so on. Few-shot object detection (FSOD) requires the model to detect objects of novel classes only through a few support images. The existing methods [17, 18, 19, 20] based on meta-learning adopt parallel structure, and extract features from support images and query images at the same time. The predictions of classification and regression are completed by using the features of the query images (or Region of Interest, RoI) combined with support features. Therefore, their relevance to each other becomes particularly important. However, some works only consider to increase the inter-class diversity in support data [17], or learn the metric to predict similarity between RoI features [19]. The relationship between support and query features remains unexploited.

As shown in Fig. 1, previous methods are to train on base classes with sufficient samples, and fine-tune the trained base model on novel classes with a small number of samples. Due to limited samples of novel classes, it is difficult to let the model learn the generalized features, which leads to erroneous classification. To better transform the knowledge of base model to novel classes, we propose in this paper to exploit the

relationship between support and RoI features to enhance the feature learning process. In other words, the dependency established between support data and RoI will make the model more discriminative.

Meanwhile, deep metric learning aims to get more generalized features according to the relations of samples. Inspired by that, we propose a dynamic relevance learning model by exploiting the similarities between features using a dynamic GCN. As illustrated in Fig. 1, the proposed model firstly projects the support data and RoI in query images to the same feature space. A graph is then constructed by using the similarity between these features as the adjacency matrix. The classification probability distribution from the base detector is then used as the node embedding and updated according to the relationship between nodes. The dynamic GCN we designed in this work can not only update the probabilities, but also capture the error of the initial probability vectors. By calculating the classification loss of the output nodes of the GCN, the features of the same category of support images and RoI will become more similar, and the features of different categories will be farther apart.

II. RELATED WORKS

The dynamic relevance learning (DRL) proposed in this paper is aim to improve the performance of few-shot object detection, which is a subproblem in few-shot learning. The idea of deep metric learning is applied to constrain the distances between visual features, with the help of a dynamic GCN bridging the support and query images.

A. Few-Shot Learning

Since deep learning based models require a large number of training samples, the models may fail to find the optimal parameters if the training data is insufficient. Most of few-shot learning algorithms introduce a suitable prior knowledge using meta-learning to narrow the space for model parameter adjustment with few samples [21].

The most direct way to address the issue of insufficient training samples is to generate new ones, [2, 3, 4] use data augmentation or Generative Adversarial Networks (GAN) to generate more samples. In order to better transfer knowledge to new tasks, [5, 6] uses additional memory to save the previous information. For the images of novel classes, similar information will be searched in the memory to help identify them. Meanwhile, other parameter adjustment based methods [7, 8, 15] try to make the model learn to get an appropriate initialization parameter for specific tasks. Metric learning based methods [9, 10, 11, 14] calculate the similarity between query and support images of each category to get the predicted category probability. Inspired by this idea, this paper proposes a dynamic GCN to further utilize the relationship between them to constrain the learning of visual features.

B. Few-Shot Object Detection

Object detection is a challenging problem in computer vision. At present, the deep learning models [22] have gradually replaced the traditional machine learning methods, and become

the mainstream algorithms in the field of object detection. Most of the algorithms can be divided into two categories, namely one stage models [23, 24, 25] and two-stage models [26, 27, 28, 29], by whether there is a separated process of region proposals.

In recent years, how to use a small number of samples for object detection has become an active topic. RepMet [30] is the first framework for few-shot object detection, which simply replaces the classification head of the traditional two-stage detection algorithm with the classification method of Matching Network [11]. LSTD [31] proposes a framework transferring knowledge that the model has learned to the novel classes. MetaYOLO [20] uses the information of support images to get the class-attentive vectors, which guide the query images to complete the detection task. MetaDet [32] decomposes the parameters of the detector into two parts, namely category-agnostic and category-specific. Meta R-CNN [17] combines class-attentive vectors with RoI feature instead of the whole image feature to make the object recognition more accurately. TFA [33] proposes a simple method based on a fine-tune process, which achieves pleasurable results in the case of few samples. The detector used in this paper is also based on meta-learner like Meta R-CNN [17], but a dynamic relevance learning model is proposed to establish a stronger link between support and query (RoI) features.

C. Deep Metric Learning

Many deep metric learning (DML) methods have been widely used in the field of FSOD, such as [19, 30, 34]. DML aims to utilize the neural networks to obtain features with strong discrimination through a simple metric function constraint. In the same embedding space, the distance between samples of the same categories becomes smaller, while the distance between samples of different categories is enlarged. Contrastive loss [35] introduces metric learning into deep neural network for the first time. To be specific, samples are paired in pairs to reduce the distance between samples within the same category and maintain a certain distance for different categories. Triplet loss [36] further considers the relationship between inter-class pairs as well as intra-class pairs. Meanwhile, many latest works focus on improving the sampling strategy [37, 38] for DML. Especially, the proxy-based methods [39, 40, 41] have attracted extensive attention due to its capability to alleviate the difficulty of sampling. Recently, group loss [41] has been proposed to take some samples of mini-batch as anchors and constrain their distances with other samples. The class probabilities are iteratively updated in an empirical way to exploit the similarities between features. However, such method may introduce undesirable bias, if the initial probability distribution is inaccurate which is often true unfortunately. The error will be accumulated after several iteration and lead to worse performance. To address this issue, we propose a more sophisticated model using a dynamic GCN to process the features from different categories.

D. Graph Convolutional Network

The graph convolutional neural network (GCN) plays a key role in the proposed DRL model. Traditional CNN can only

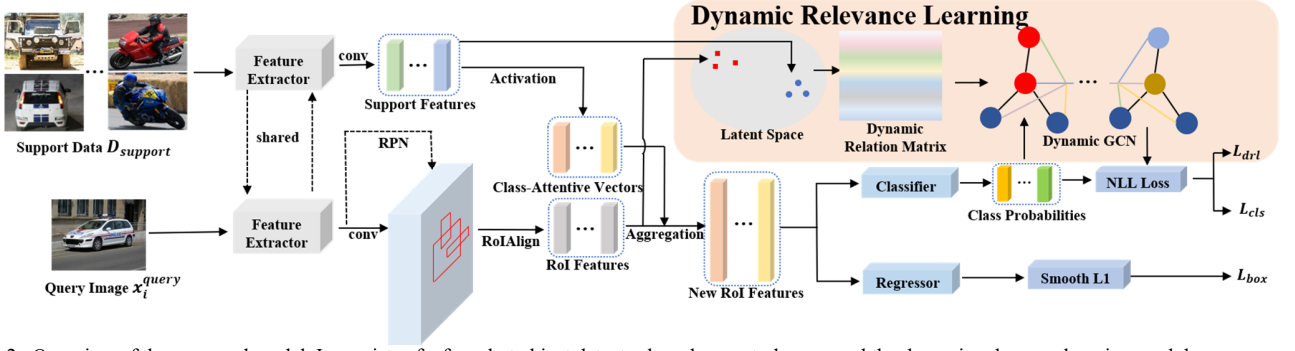


Fig. 2. Overview of the proposed model. It consists of a few-shot object detector based on meta-learner and the dynamic relevance learning module.

process Euclidean spatial data, but in real life most of the data is in the form of graph data. Migrating CNN to analysis and process graph data, GCN was first proposed in [42] to address the semi-supervised classification problem. Subsequently, many improvements of GCN have been proposed [43, 44].

Recently, there is a new trend that utilizing GCN to help models in recognition tasks. To obtain better representation of video content, a Dual-Pooling GNN is proposed in [12]. In Zero-shot learning, GCN is used in [45] with semantic embeddings and categorical relationships of knowledge graph to predict the classifiers. To improve the categorical relationships, a Dense Graph Propagation (DGP) module is proposed in [46]. Furthermore, a novel ML-ZSL approach [47] is proposed to explore the associated structured knowledge. In [48], GCN is introduced to form the attribute propagation network (APNet). In zero-shot detection, GCN has also been used in Semantics-Preserving Graph Propagation model (SPGP) [49]. It can effectively use the semantic embeddings and structural knowledge given in the previous category diagram to enhance the generalization ability of the learned projection function.

Most of the aforementioned works generate a static graph for GCN in advance based on the relationships between categories. However, due to the changing of data in some cases, different graph structures may need to be established during the training. In such case, dynamic GCN [50] is required. Unfortunately, very few related researches have been reported. In this paper, a new type of dynamic GCN is proposed for deep metric learning.

III. METHODOLOGY

In the task of Few-Shot Object Detection (FSOD), the dataset is usually divided into two parts: base classes C_{base} with large number of samples n_{base} and novel classes C_{novel} with only a few samples n_{novel} , where $n_{base} \gg n_{novel}$. The corresponding data of these two categories are denoted as D_{base} and D_{novel} . The goal of FSOD is to train a detector $h(\cdot; \theta)$ on D_{base} and quickly adapt this detector to D_{novel} . θ is the learnable parameter in this detector. However, extreme data imbalance will make the model vulnerable to overfitting on the D_{novel} . Thus, meta-learning [17-20, 32] has been proposed to address this issue.

In meta-learning, a subset $C_{meta} \in C_{base} \cup C_{novel}$ is extracted from the base and novel classes during each training iteration. These samples in C_{meta} are then re-divided into training data $D_{query} = \{(x_i^{query}, y_i^{query})\}_{i=1}^{n_q}$ and category

information $D_{support} = \{(x_{c,k}^{support}, y_{c,k}^{support})\}_{c=1}^{n_{meta}} \{k=1\}^K$, where n_q and n_{meta} are the number of query images in the mini-batch and categories in $D_{support}$ respectively. Since there are only a small amount of samples (K images from D_{base} or D_{novel}) in each category, the model $h(x_i^{query}; D_{support}; \theta)$ is capable of adapting to D_{novel} effectively. As shown in Fig. 2, x_i^{query} and $D_{support}$ represent the query images and support data, respectively. However, the above meta-learning paradigm does not make full use of the support data. Only the support data is utilized to obtain class-attentive vectors in the original Meta R-CNN [17]. In this paper, we propose a novel Dynamic Relevance Learning to further explore the relevance between the support features and the query features.

A. Overview of Our Model

As shown in Fig. 2, our framework is mainly divided into two parts, the detector based on meta-learner $h(\cdot; D_{support}; \theta)$ and the Dynamic Relevance Learning responsible for associated learning between support features and query features. The detector utilizes convolutional neural networks (CNNs) as the feature extractor to simultaneously generate the feature maps from the support data $D_{support}$ and query image x_i^{query} . Then, the Region Proposal Network (RPN) [28] and RoIAlign [29] are used to obtain the RoI features $\{r_{i,j} \in \mathbb{R}^f\}_{j=1}^{n_{roi}}$ from the query feature map. The average value of K sample features in support data $D_{support}$ corresponding to class $c \in C_{meta}$ is used as the class representation. Then the class-attentive vector $a_c \in \mathbb{R}^f$ is obtained as,

$$v_{c,k} = F^{exr}(x_{c,k}^{support}) \quad (1)$$

$$a_c = \delta\left(\frac{1}{K} \sum_{k=1}^K v_{c,k}\right) \quad (2)$$

where $F^{exr}(\cdot)$ denotes the feature extractor (i.e. CNNs), $v_{c,k}$ is the support features of the k -th image in c -th category and $\delta(\cdot)$ presents the sigmoid activation function.

The class-attentive vector a_c and the RoI feature $r_{i,j}$ are then aggregated and fed into the prediction head. The aggregation operation \mathcal{A} proposed in [18] is adopted in our model to obtain the new RoI feature $\hat{r}_{i,j} \in \mathbb{R}^{2f}$,

$$\begin{aligned} \hat{r}_{i,j} &= \mathcal{A}(a_c, r_{i,j}) \\ &= [r_{i,j} \otimes a_c; r_{i,j} \ominus a_c; r_{i,j}] \end{aligned} \quad (3)$$

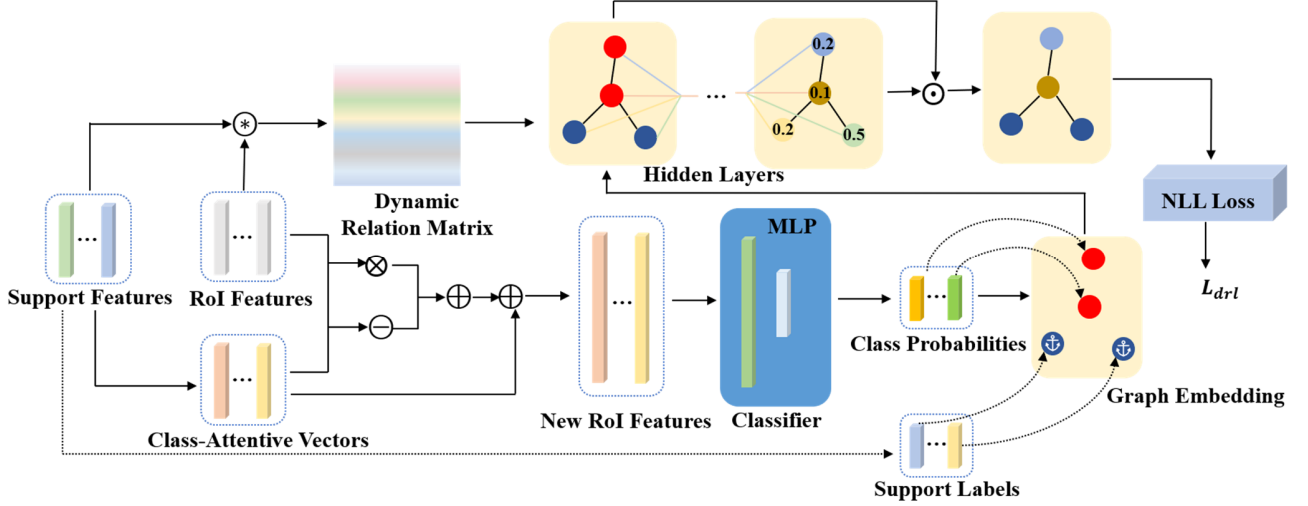


Fig. 3. Dynamic relevance learning. \otimes and \ominus represent channel-wise multiplication and subtraction, respectively. \oplus denotes concatenation operation, \odot calculates the Pearson's correlation coefficient, and \odot is node-wise multiplication.

where \otimes , \ominus and $[\cdot]$ represent channel-wise multiplication, subtraction and concatenate operation, respectively. Then the classification probability distribution $\{p_{i,j}\}_{j=1}^{n_{roi}}$ is calculated by the classification head through the new RoI features $\{\hat{r}_{i,j}\}_{j=1}^{n_{roi}}$.

$$p_{i,j} = \text{softmax}(F^{cls}(\hat{r}_{i,j})), \quad p_{i,j} \in \mathbb{R}^{n_{meta}} \quad (4)$$

where $F^{cls}(\cdot)$ represents the classification head function which is a Multi-Layer Perception (MLP) in this work. At the end, the classification loss L_{cls} and regression loss L_{reg} can be obtained through the $\{p_{i,j}\}_{j=1}^{n_{roi}}$, $\{\hat{r}_{i,j}\}_{j=1}^{n_{roi}}$ and the labels.

Although meta-learning has alleviated the data imbalance problem between the C_{base} and C_{novel} , the detection performance on D_{novel} is still unsatisfactory. The main reason is that the limited support samples from D_{novel} lead to unstable class representation. Moreover, such unstable representation may introduce confused information in the RoI learning stage, since $v_{c,k}$ is aggregated into the RoI feature $\hat{r}_{i,j}$.

To address this issue, we propose a Dynamic Relevance Learning paradigm. The key concept is using the dependency (between support and RoI features) modeled by a dynamic GCN to improve the class representation implicitly. Specifically, the support features and RoI features are mapped to a latent space, while their similarity matrix is adopted as the adjacency matrix of dynamic GCN. The previous class probabilities $\{p_{i,j}\}_{j=1}^{n_{roi}}$ and the support data labels $\{y_{c,k}^{support}\}_{c=1; k=1}^{n_{meta} K}$ are utilized as the node embeddings in the graph convolution. This dynamic GCN is further constrained by the classification loss L_{drl} of the node embeddings during the training stage. The details of this dynamic relevance learning will be discussed in the next section.

B. Dynamic Relevance Learning

When transferring the base model trained on D_{base} with sufficient samples to D_{novel} with only limited samples, it often suffers a great performance degradation. This is obviously due to the lack of samples that makes the model struggling to learn

the desirable feature representation. In most frameworks of meta-learning, the support data $D_{support}$ provide general class-attentive vectors, which are equivalent to the category templates for RoI learning. To further explore the relation between the support and RoI features, a dynamic relevance learning paradigm is proposed to build proper connections between them. Two types of dynamic GCN are designed to adjust the prediction classification probability distribution, which guides the feature representation learning implicitly. Each node embedding in GCN is updated according to the nodes connected with it. Thus, it is naturally suitable to model the relevance between categories.

Given a graph $G = \{V, E, A\}$ for constructing GCN, V and E are the sets of nodes and edges respectively and A is the adjacency matrix indicating the relationship between each node. In our task, the nodes $V = \{V_s, V_q\}$ represent either the support images (V_s) or RoIs (V_q) from the query image x_i^{query} . As shown in Fig. 3, the similarity matrix S of support features $\{v_{c,k}\}_{c=1; k=1}^{n_{meta} K}$ and RoI features $\{r_{i,j}\}_{j=1}^{n_{roi}}$ is adopted as the adjacency matrix of graph G , which is calculated using Pearson's correlation coefficient,

$$s_{ij} = \frac{\text{Cov}(v_i, r_j)}{\sqrt{\text{Var}(v_i, r_j)}} \quad (5)$$

where s_{ij} is the element of matrix S . It is worth noting that, in conventional GCNs, the graph G is determined before the training stage and such graph structure will not be altered throughout the whole training process. However, the support data $D_{support}$ and the query image x_i^{query} changes at each training iteration. In other words, the graph G keeps changing during the training process. Thus, instead of building a static graph in advance, the dynamic GCN is employed to learning the dynamic relevance between the altering nodes, while matrix S is now viewed as a dynamic relation matrix.

Inspired by group loss [41], a small portion of samples are selected as anchor nodes in each training mini-batch, while the rest are denoted as drift nodes. The output of these anchor nodes is identical to their input node embeddings, i.e., the labels,

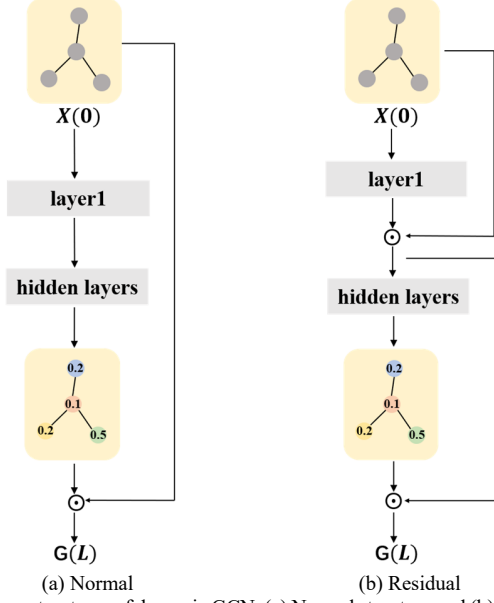


Fig. 4. Two structures of dynamic GCN, (a) Normal structure and (b) Residual structure. \odot Represents the multiplication of the corresponding nodes.

which provide a strong guidance for the drift nodes. Specifically, as shown in Fig. 3, the support images (V_s) are chosen as anchor nodes, while the one-hot coded support labels $y_{c,k}^{support}$ and the RoI classification probabilities $p_{i,j}$ are considered as the node embeddings for V_s and V_q , respectively. Since the labels of support data are well-labeled, they can produce a reliable guiding effect for RoI feature learning. To be noted, the RoI features (V_q) generated by RPN are not suitable to be the anchor nodes, because either their position or category classification are inaccurate.

According to the dynamic relation matrix S , the anchor and drift nodes and their corresponding node embeddings, the input $X(0)$ of the proposed dynamic GCN is,

$$X(0) = \{p_{i,j}\}_{j=1}^{n_{roi}} \cup \{y_{c,k}^{support}\}_{c=1; k=1}^{n_{meta} K} \quad (6)$$

In order to make the graph convolution calculation process smoother. Formally, the graph convolution is defined as,

$$Z(l) = \sigma(SX(l)W(l)) \quad (7)$$

where $l = 1, 2, 3, \dots, L$ is the layer index of GCN, $X(l)$ is input of layer l , $W(l) \in \mathbb{R}^{n_{meta} \times n_{meta}}$ is the learnable weight matrix of layer l , σ is a non-linear activation function, and $Z(l)$ is the output of layer l .

The output $Z(L)$ of the L -th layer is considered as the relevance attention to indicate the confidence on each category according to the input node embedding and connected nodes. As shown in Fig. 4. (a), these weights are multiplied back to the initial input $X(0)$ to get the updated node embeddings $G(L)$,

$$G(L) = Z(L) \odot X(0) \quad (8)$$

In such manner, the original probability distribution $\{p_{i,j}\}_{j=1}^{n_{roi}}$ will be modified based on the relevance attention $Z(L)$, which is determined by the relation between RoI and support features. This structure is slightly different from the traditional GCN,

since we found it performs better to learn the attention scores instead of a modified probability distribution directly.

To consider the over-smoothing issue in GCN, we propose the other residual-like structure of GCN, as shown in Fig. 4 (b). Instead of directly using $Z(l)$ (the output of l -th layer) as the input of next layer, $X(l+1)$ is obtained by multiplying $Z(l)$ by the input of l -th layer $X(l)$ as,

$$X(l+1) = Z(l) \odot X(l) \quad (9)$$

According to the experimental results, the performance of residual structure is generally better than the normal structure if there are adequate samples. More detailed discussion will be given in Section IV.

The output $G(L)$ of GCN as the enhanced probability is then used to calculate the loss through Cross Entropy function. Formally, the loss L_{drl} is defined as

$$L_{drl} = -\frac{1}{n_{roi}} \sum_{i=1}^{n_{roi}} y_i^{query} \log g_i(L) \quad (10)$$

where $g_i(L)$ is i -th node embedding of $G(L)$.

This loss adds implicit constraints between the RoI and support features. If a certain pair of RoI and support features shares a high similarity s_{ij} , strong link will be made between these two kinds of nodes (anchor and drift nodes). As a result, the drift node tends to give a high confidence at the same category the anchor node belongs to, which makes the predicted probability distribution close to the support label. If this prediction is correct, L_{drl} will be small. Otherwise, it gives penalty on such wrong relevance, which will encourage the model to increase the gap between them in the visual feature space.

C. Training strategy

The training process can be divided into two stages. The first stage uses a large amount of base class data to train the model, and the second one adopts a small amount of mixed data of novel and base classes. Due to the large difference in the data amount between these two stages, different loss functions are employed. Formally, the loss of base training L_{base} is defined as,

$$L_{base} = L_{rpn} + L_{cls} + L_{box} + L_{meta} + L_{drl} \quad (11)$$

where L_{rpn} is proposed in Faster-RCNN [28] for training RPN with better proposals. L_{cls} and L_{box} are proposed in Fast-RCNN [27] to train the classification and regression head. L_{meta} is proposed in Meta R-CNN [17] to get more stable support representation. L_{drl} is proposed in last section to establish proper relevance of support features and RoI features.

The meta loss L_{meta} has a relatively simple form designed to diversify the inferred object attentive vectors. It works well if there are sufficient training samples. However, it may cause the support features deviate from the true representation, if only few samples are available in the fine-tune phase. Therefore, the meta loss L_{meta} is not applied in the fine-tune phase. Formally, the loss of fine-tune phase L_{tune} is defined as,

$$L_{tune} = L_{rpn} + L_{cls} + L_{box} + L_{drl} \quad (12)$$

TABLE I
EVALUATION RESULTS ON PASCAL VOC 2007 TEST SET (AP50, %)

Method \ Shot	Novel Set 1					Novel Set 2					Novel Set 3				
	1	2	3	5	10	1	2	3	5	10	1	2	3	5	10
LSTD [31]	8.2	1.0	12.4	29.1	38.5	11.4	3.8	5.0	15.7	31.0	12.6	8.5	15.0	27.3	36.3
MetaYOLO [20]	14.8	15.5	26.7	33.9	47.2	15.7	15.2	22.7	30.1	40.5	21.3	25.6	28.4	42.8	45.9
MetaDet [32]	18.9	20.6	30.2	36.8	49.6	21.8	23.1	27.8	31.7	43.0	20.6	23.9	29.4	43.9	44.1
Meta R-CNN[17]	19.9	25.5	35.0	45.7	51.5	10.4	19.4	29.6	34.8	45.4	14.3	18.2	27.5	41.2	48.1
TFA [33]	25.3	36.4	42.1	47.9	52.8	18.3	27.5	30.9	34.1	39.5	17.9	27.2	34.3	40.8	45.6
FSDVE [18]	24.2	35.3	42.2	49.1	57.4	21.6	24.6	31.9	37.0	45.7	21.2	30.0	37.2	43.8	49.6
DRL (normal)*	30.3	40.8	49.1	48.0	58.6	22.4	36.1	36.9	35.4	51.8	24.8	29.3	37.9	43.6	50.4
DRL (residual)*	28.0	40.5	49.4	49.9	59.4	22.9	33.4	36.4	36.1	52.7	28.0	32.0	40.4	46.7	53.5

* The reported results are the average of 10 random runs.

TABLE II
AP OF DIFFERENT CLASSES ON VOC NOVEL SET 2

Shot	Method	Classes				
		aeroplane	bottle	cow	horse	sofa
1	FSDVE* [18]	35.8	0.3	31.0	10.6	30.0
	DRL (residual)	36.8	8.5	25.3	15.1	28.8
3	FSDVE* [18]	47.6	0.4	48.9	29.5	44.1
	DRL (residual)	44.5	5.7	49.3	35.5	46.7
5	FSDVE* [18]	50.5	0.9	53.9	41.0	41.5
	DRL (residual)	43.9	2.9	50.2	35.0	48.4
10	FSDVE* [18]	55.8	15.1	56.7	66.1	50.2
	DRL (residual)	52.9	21.1	63.9	72.1	53.6

*The reported results come from the official code. The mAPs are slightly higher than the ones reported in their paper [18] shown in Table I.

In addition, removing L_{drl} from (11) in the base training stage will not affect the performance on D_{novel} too much. In the inference stage, we simply use the original probability distribution $\{p_{i,j}\}_{j=1}^{n_{roi}}$ for classification. Even without the dynamic relevance learning part, the performance is still improved due to better feature representation learned in the training stage.

IV. EXPERIMENTS

In this section, the experimental results on Pascal VOC [51] and MS-COCO [52] dataset of the proposed dynamic relevance learning are presented, which are also compared with the state-of-the-art methods. Ablation studies and detailed analysis are also included.

A. Benchmarks and Setups

To make a fair comparison, our experimental setups on Pascal VOC 2007, 2012 [51] and MS-COCO 2014 [52] datasets are consistent with [17, 18, 20]. Following the description in [20], three different schemes are utilized to take five classes as novel classes from the original Pascal VOC dataset (20 object categories in total) to perform few-shot detection. Each class has only K pictures to participate in the fine-tune training stage, $K = 1, 2, 3, 5, 10$. The remaining 15 classes are base classes, providing sufficient samples to participate in both the base and fine-tune training stages. MS-COCO dataset is a more challenging dataset, which contains 80 categories in total. Among them, 20 categories belonging to Pascal VOC are regarded as novel classes, and the other 60 categories are

regarded as base classes.

B. Analysis of experimental results

1) Pascal VOC

The experimental results are presented in Table I. It can be seen that the proposed model with two GCN structures (normal and residual ones) achieves the highest accuracy in almost all the setups with three different partitions of dataset and different number of novel class samples. Compared with State-Of-The-Art (SOTA) method FSDVE [18], our model shows constant improvement in term of AP50, except the 5-shot setting in novel set 2.

Since different novel sets contain different novel classes, the performance varies from set to set. For example, in the Novel Set 1, the five novel classes are “bird, bus, cow, motorbike, sofa”. The biggest improvement is 7.2% in the 3-shot setting of residual structure. However, in the 5-shot setting, the improvement is relatively minor (0.8% for the residual structure), which leads to very close result in our model of 3-shot and 5-shot. Although it performs well when there are only limited samples, the performance does not scale linearly when the number of samples is increased from 3 to 5. The similar cases can be found in Novel Set 2.

In Novel Set 2 with the novel classes “aeroplane, bottle, cow, horse, sofa”, the AP50 from 3-shot to 5-shot decrease 0.3% of residual structure. The best guess is that the proposed DRL model is less effective at handling small objects compared to medium and large ones, which can be observed in the MS-COCO experiments as well. Moreover, in the AP50 of each category shown in Table II, the smallest object “bottle” has the worst performance for both the proposed DRL and FSDVE [18]. The main reason is that the support and query images of “bottle” usually contain a more complicated image background, such as a cluttered desktop. Noting that our DRL model still outperforms the compared method, thanks to the relationship between the features built by the dynamic GCN. Despite this, the proposed DRL model shows noticeable performance on 1, 2, 3-shot detection. In the 10-shot setting, the DRL gets improvement up to 7.0% when each category gets stable representation.

In contrast, the accuracy of DRL scales well with the sample numbers and constantly higher than the SOTA method FSDVE

TABLE III
EVALUATION RESULTS ON MS-COCO 2014 DATASET (%)

Shot	Method	AP	AP ₅₀	AP ₇₅	AP _S	AP _M	AP _L	AR ₁	AR ₁₀	AR ₁₀₀	AR _S	AR _M	AR _L
10	LSTD [31]	3.2	8.1	2.1	0.9	2.0	6.5	7.8	10.4	10.4	1.1	5.6	19.6
	MetaYOLO [20]	5.6	12.3	4.6	0.9	3.5	10.5	10.1	14.3	14.4	1.5	8.4	28.2
	MetaDet [32]	7.1	14.6	6.1	1.0	4.1	12.2	11.9	15.1	15.5	1.7	9.7	30.1
	Meta R-CNN[17]	8.7	19.1	6.6	2.3	7.7	14.0	12.6	17.8	17.9	7.8	15.6	27.2
	TFA [33]	9.1	17.1	8.8	-	-	-	-	-	-	-	-	-
	FSDVE [18]	10.5	25.5	5.7	4.0	11.4	14.7	18.6	23.8	23.9	8.8	25.4	32.2
	DRL (normal)*	11.9	27.4	7.9	3.8	12.6	17.7	19.7	25.2	25.3	8.6	26.7	35.5
	DRL (residual)*	10.9	25.2	7.0	3.6	11.2	16.0	19.0	24.7	24.7	8.1	25.7	34.4
30	LSTD [31]	6.7	15.8	5.1	0.4	2.9	12.3	10.9	14.3	14.3	0.9	7.1	27.0
	MetaYOLO [20]	9.1	19.0	7.6	0.8	4.9	16.8	13.2	17.7	17.8	1.5	10.4	33.5
	MetaDet [32]	11.3	21.7	8.1	1.1	6.2	17.3	14.5	18.9	19.2	1.8	11.1	34.4
	Meta R-CNN[17]	12.4	25.3	10.8	2.8	11.6	19.0	15.0	21.4	21.7	8.6	20.0	32.1
	TFA [33]	12.1	22.0	12.0	-	-	-	-	-	-	-	-	-
	FSDVE [18]	14.6	31.2	11.4	5.3	15.3	21.8	22.3	29.3	29.5	11.4	31.4	39.1
	DRL (normal)*	14.6	31.3	11.3	4.8	15.5	22.3	22.1	28.7	28.8	10.8	30.0	40.4
	DRL (residual)*	15.0	31.7	11.8	4.8	15.9	23.1	22.6	29.6	29.7	11.1	31.0	41.3

‡ the reported results come from the official pre-training model and code.

* the reported results are the average of five random runs.

in Novel Set 3. The five novel classes are "boat, cat, motorbike, sheep, sofa", which all have moderate sizes.

2) MS-COCO

The experimental results are shown in Table III. The standard MS-COCO evaluation protocol is followed, which includes mean Average Precision (AP) with different Intersection over Union (IoU) with ground truth, and AP with objects occupying areas of different sizes. At the same time, we also add mean Average Recall (AR) with different top proposals as a measure. So that we can evaluate the model performance more comprehensively. Compared with Pascal VOC, the improvement on MS-COCO is relatively small, because the images in MS-COCO is more complex and has more categories and samples.

Compared with the SOTA method FSDVE, in the 10-shot setting, our method has about 1.0%-1.3% improvement in both AP and AR, which shows the effectiveness of the proposed DRL. Similarly, we found that the results on small objects are slightly lower (-0.2%) than the SOTA method. However, there is a great improvement on large objects (over 2% boost in AP_L and AR_L). This is actually an inherent problem in deep metric learning. We need to constrain the features by the distance between RoI and support features, in order to obtain more generalized features to help improve recognition performance. However, for small objects, the semantic information of the feature itself is not clear enough. Due to this, the constraint of feature distance may make it move in the wrong direction.

In the 30-shot setting, the overall performance of DRL is still superior to the SOTA methods, with at least 0.2%-0.4% improvement in AP and AR. At the same time, DRL is still not good at the detection of small objects. This also confirms the above analysis, small objects could cause semantic deviation, which may become more serious when the number of samples becomes more.

TABLE IV
COMPARISONS OF THE META LOSS AND DRL (MS-COCO 10-SHOT, %)

Meta loss	DRL	AP	AP ₅₀	AR ₁	AR ₁₀
		11.1	26.3	18.8	24.8
√		10.5	25.5	18.6	23.8
	√	11.9	27.4	19.7	25.2
√	√	10.9	26.1	19.2	24.7

The reported results are obtained using DRL (normal).

C. Ablation study

1) Two structures of GCN

The results of two proposed GCN structures, namely normal and residual GCN, have been presented in Tables I and III. It can be seen that, in 1 or 2-shot settings in PASCAL VOC and 10-shot setting in MS-COCO, the performance of normal GCN is higher than that of the residual GCN. With such few samples, support images cannot provide stable class representation. In the same time, support features are used to update the prediction probability more frequently in the residual GCN. Inaccurate class representation will make the error further expand, and normal structure can alleviate this situation.

As the number of samples increase (5-10 shots in PASCAL VOC or 30 shots in MS-COCO), the performance of the residual GCN has been noticeably improved. This difference shows the number of anchor nodes is important for the proposed dynamic relevance learning. It is because the amount of available support features indicates how many direct connections with strong relevance between nodes are available. Moreover, the residual structure may be able to alleviate the inaccurate influence between drift nodes (RoI features).

2) Influence of the meta loss

Meta loss was first proposed in Meta R-CNN [17], which is a simple but effective way. The Cross Entropy function is used

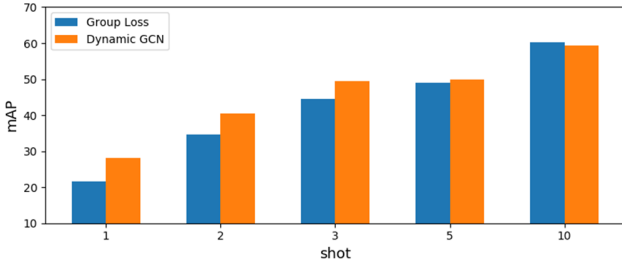


Fig. 5. The comparisons between Group Loss and dynamic GCN on the VOC Novel Set 1. The results are obtained using DRL (residual).

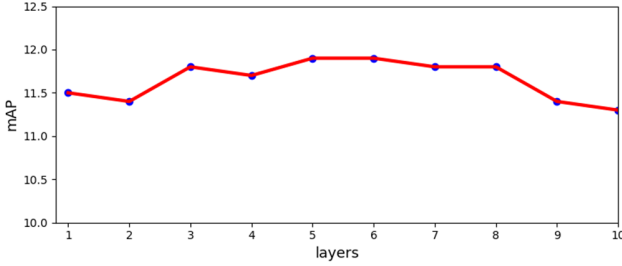


Fig. 6. The effect of different depths of GCN in MS-COCO 10-shot setting. The results are obtained using DRL (normal).

to calculate the loss of image classification in support set, trying to expand the distance between inter-classes, so that different categories have diverse effects on query images. However, in our experiments, we find that meta loss is not suitable for the fine-tune training stage as stated in Training strategy.

As shown in Table IV, with and without the meta loss, the AP of novel classes has about 0.6% difference. The combination of the meta loss with the proposed DRL will also degrade the performance. The best guess is that the meta loss forced classification constraint on a certain class, instead of directly adding constraints to the distance between features. When there are enough samples, this method can make the features of different categories more diversity. But in case of very few samples, which may make the representation of the class deviate and thus cannot represent the class well. Our DRL still shows good performance even in the case of insufficient samples.

3) Comparisons between the Group Loss and Dynamic GCN

The proposed DRL model is inspired by Group Loss [41]. It iterates the initial class probabilities $\{p_j\}_{j=1}^{n_{roi}}$ of all RoI in a fixed way through the feature distance S between samples,

$$\pi_{i,c} = \sum_{j=1}^N S_{ij} p_{j,c} \quad (13)$$

where $\pi_{i,c}$ can be regarded as the confidence that RoI feature r_i belongs to class c , which is determined by the similarity S_{ij} between i -th and j -th samples as well as the probability of the j -th sample for class c . Then the enhanced probability of $r_{i,c}$ for class c can be obtained by multiplying the confidence $\pi_{i,c}$ and initial probability $p_{i,c}$ with a normalization step,

$$r_{i,c}(t+1) = \frac{r_{i,c}(t)\pi_{i,c}(t)}{\sum_{\mu} r_{i,\mu}(t)\pi_{i,\mu}(t)} \quad (14)$$

Shot	Base (mAP)			Novel (mAP)		
	1	2	10	1	2	10
Base training + Fine-tune	62.3	64.3	68.5	28.6	40.3	59.4
Only Fine-tune	59.7	62.8	67.9	28.0	40.5	59.4

The reported results are obtained using DRL (residual).

Shot	1	2	3	5	10
image + mask	28.1	41.9	47.4	49.9	58.4
instance	28.0	40.5	49.4	49.9	59.4

The reported results are obtained using DRL (residual).

where t indicates t -th iteration, and $r_{i,c}(0) = p_{i,c}$.

The comparisons are demonstrated in Fig. 5. The results of the group loss are inferior to DRL in 1, 2, 3 and 5-shot detection. In the case 10-shot, group loss and DRL obtain very close results. With 10 or more samples per class, the model could get more stable category representation. Therefore, the fixed iteration method can also establish reliable connection between support data and query images, although the number of iterations still need to be determined manually.

4) Base training with DRL

To show the effectiveness of DRL in different training stages, the results with and without DRL in base training stage are given in Table V. It can be seen that using DRL solely in the fine-tune stage can produce good enough results for the novel classes. But for base classes, utilizing DRL can further push the AP up of 1.5%-2.6%. It also reflects that the proposed DRL can help pre-trained model to quickly adapt to new tasks.

5) Different input format of support images

To get clearer object information, there are generally two input formats for support images. One contains only the instance, i.e. the object part in the image. The other provides the whole 3-channel image with a binary mask channel, while the instances and background are marked as 1 and 0, respectively. The influence of the input format has been discussed in MetaYOLO [20], and the conclusion is that adding binary mask will bring about 2% AP improvement. In this paper, we show different results with the proposed DRL. As given in Table VI, the whole image + mask is better in 1 and 2-shot settings, while its performance is inferior to the instance in 3 and 10-shot settings.

The reason of such difference may be that the feature extractors of support and query images in MetaYOLO [20] do not share parameters. Hence, the addition information in the mask channel may help the feature extraction of support images, which leads to a better performance. In contrast, the feature extractors of the proposed DRL model have the same parameters, while the dynamic GCN introduces further information exchange.

6) Different number of layers in dynamic GCN

The number of model layers is always a vital hyper-

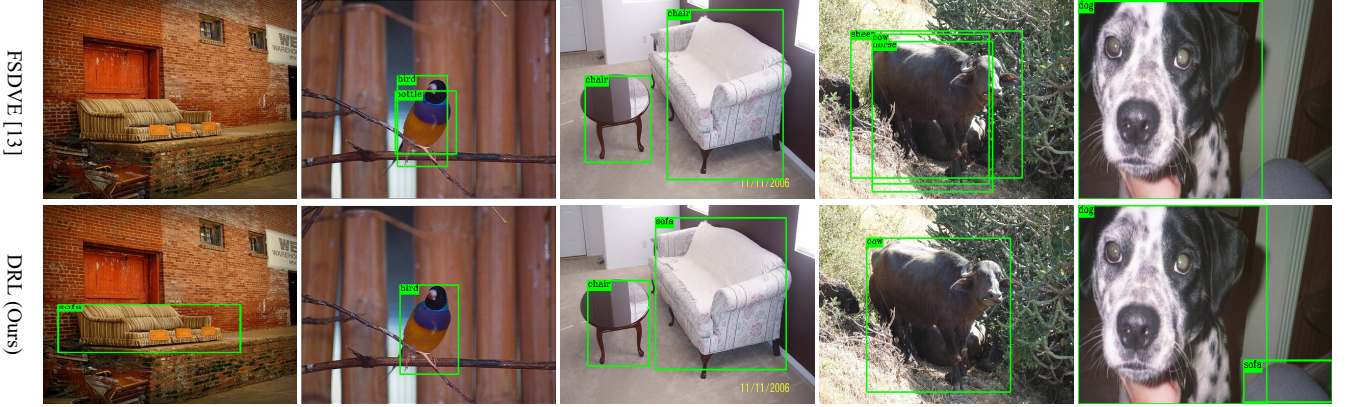


Fig. 7. The visualization of novel classes objects on VOC Novel Set 1 detected by FSDVE [18] and our DRL, the structure of GCN is Residual

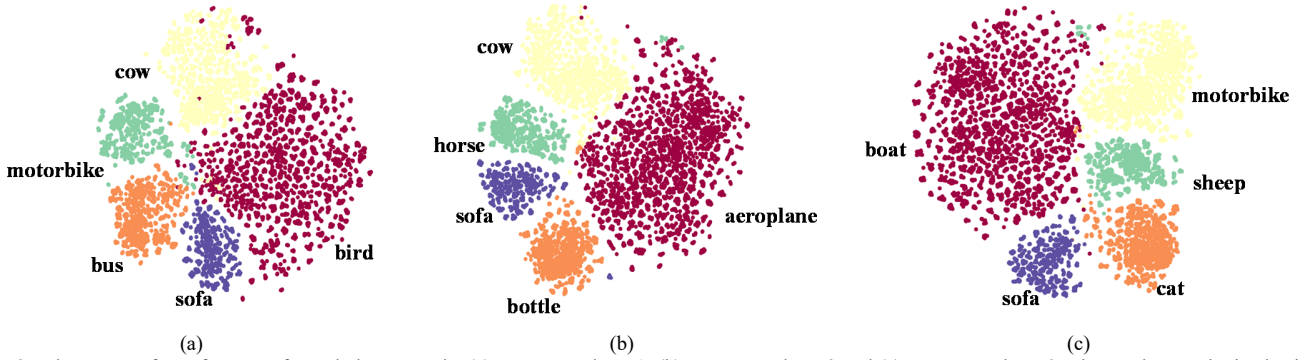


Fig. 8. The t-SNE of RoI features of novel classes on the (a) VOC Novel Set 1, (b) VOC Novel Set 2 and (c) VOC Novel Set 3. The results are obtained using DRL (residual) in 10-shot setting.

parameter. The network structure of traditional GCNs is much shallower than CNNs. In the proposed DRL, the dynamic GCN is employed which is more complicate than the static one. Thus, the effect of different depths for normal dynamic GCN structure is given in Fig. 6. It can be seen that the performance improves slightly when the number of layers increasing from 1 to 6. After the number exceed 7, the performance starts declining gradually. In other words, the performance is not very sensitive to the number of layers for the proposed DRL model.

D. Visualization of the detection results

To demonstrate the superiority of DRL more intuitively, we visualize several detection results of five novel classes on VOC Novel Set 1 in Fig. 7. In the first and fifth pictures, the appearance of the sofa is like the background, thus FSDVE [18] mistakenly classifies it as the background. In the fine-tuning phase, our DRL uses the support feature as a reference to adjust the sample features, resulting a greater distance between the background and object features of RoI, which leads to better results. The second to the fourth contain similar mistakes for FSDVE. Although the object is correctly located and classified, the background is mistakenly classified as the foreground object. In contrast, our model can alleviate such problem effectively.

E. Visualization of RoI features

RoI features learned by DRL are visualized using t-SNE [53] in Fig. 8, which can provide a more intuitively observation of the relationship between different classes of features. It can be seen that the RoI features of the same category are well

clustered, and there are obvious boundaries between different categories. This shows that DRL is effective to constrain the learning of RoI features by using the support features as guidance information. Meanwhile, it is also capable to learn the correct semantic information when there are only 10 training samples in each category.

V. CONCLUSION

In this paper, to improve the performance of few-shot object detection, we have proposed a dynamic relevance learning model, which can guide the learning of category representation by utilizing the relationship between the support and query images. Two types of dynamic GCNs have been constructed and tested, which take the embeddings of the sample as the graph node and update the information by graph convolution. The experimental results and ablation study show that the DRL is effective in FSOD, due to its ability to learn more generalized features.

REFERENCES

- [1] K. He, X. Zhang, S. Ren and J. Sun, "Deep Residual Learning for Image Recognition," in *Proc. IEEE Conf. Comput. Vision Pattern Recognit.*, 2016, pp. 770-778.
- [2] B. Hariharan and R. Girshick, "Low-Shot Visual Recognition by Shrinking and Hallucinating Features," in *Proc. IEEE Int. Conf. Comput. Vision.*, 2017, pp. 3037-3046.
- [3] A. Antreas, A. Storkey, and H. Edwards, "Data augmentation generative adversarial networks," arXiv preprint arXiv: 1711.04340, 2017.
- [4] Y. Wang, R. Girshick, M. Hebert and B. Hariharan, "Low-Shot Learning from Imaginary Data," in *Proc. IEEE Conf. Comput. Vision Pattern Recognit.*, 2018, pp. 7278-7286.

- [5] A. Santoro, S. Bartunov, M. Botvinick, D. Wierstra, and T. Lillicrap, "Meta-learning with memory-augmented neural networks," in *Proc. Int. Conf. Mach. Learn.*, 2016, pp. 1842-1850.
- [6] P. Sprechmann *et al.*, "Memory-based parameter adaptation," arXiv preprint arXiv:1802.10542, 2018.
- [7] S. Ravi, and H. Larochelle, "Optimization as a Model for Few-Shot Learning," in *Proc. Int. Conf. Learn. Representation.*, 2017.
- [8] C. Finn, P. Abbeel, and S. Levine, "Model-Agnostic Meta-Learning for Fast Adaptation of Deep Networks," in *Proc. ACM 34th Int. Conf. Mach. Learn.*, 2017, pp. 1126-1135.
- [9] J. Snell, K. Swersky, and R. Zemel, "Prototypical networks for few-shot learning," in *Proc. Adv. Neural Inf. Process. Syst.*, 2017, pp. 4080-4090.
- [10] F. Sung *et al.*, "Learning to Compare: Relation Network for Few-Shot Learning," in *Proc. IEEE Conf. Comput. Vision Pattern Recognit.*, 2018, pp. 1199-1208.
- [11] O. Vinyals *et al.*, "Matching Networks for One Shot Learning," in *Proc. Adv. Neural Inf. Process. Syst.*, 2016, pp. 3637-3645.
- [12] Y. Hu, J. Gao and C. Xu, "Learning Dual-Pooling Graph Neural Networks for Few-shot Video Classification," in *IEEE Trans. Multimedia.*, November. 2020.
- [13] Y. Zhu, W. Min and S. Jiang, "Attribute-Guided Feature Learning for Few-Shot Image Recognition," in *IEEE Trans. Multimedia.*, vol. 23, pp. 1200-1209, May. 2020.
- [14] H. Huang, J. Zhang, J. Zhang, J. Xu and Q. Wu, "Low-Rank Pairwise Alignment Bilinear Network For Few-Shot Fine-Grained Image Classification," in *IEEE Trans. Multimedia.*, vol. 23, pp. 1666-1680, June. 2020.
- [15] A. Phaphuangwittayakul, Y. Guo and F. Ying, "Fast Adaptive Meta-Learning for Few-shot Image Generation," in *IEEE Trans. Multimedia.*, May. 2021.
- [16] Z. Zheng, Z. Yu, H. Zheng, Y. Yang and H. T. Shen, "One-Shot Image-to-Image Translation via Part-Global Learning with a Multi-adversarial Framework," in *IEEE Trans. Multimedia.*, January. 2021.
- [17] X. Yan, Z. Chen, A. Xu, X. Wang, X. Liang and L. Lin, "Meta R-CNN: Towards General Solver for Instance-Level Low-Shot Learning," in *Proc. IEEE Int. Conf. Comput. Vision.*, 2019, pp. 9576-9585.
- [18] Y. Xiao *et al.*, "Few-shot object detection and viewpoint estimation for objects in the wild," in *Proc. Eur. Conf. Comput. Vision*, 2020, pp. 192-210.
- [19] T. Hsieh, Y. Lo, H. Chen, and T. Liu, "One-Shot Object Detection with Co-Attention and Co-Excitation," in *Proc. Adv. Neural Inf. Process. Syst.*, 2019, pp. 2721-2730.
- [20] B. Kang, Z. Liu, X. Wang, F. Yu, J. Feng and T. Darrell, "Few-Shot Object Detection via Feature Reweighting," in *Proc. IEEE Int. Conf. Comput. Vision.*, 2019, pp. 8419-8428.
- [21] Y. Wang, Q. Yao, J. T. Kwok, and L. M. Ni, "Generalizing from a Few Examples: A Survey on Few-shot Learning," *ACM Comput. Surv.*, vol. 53, no. 63, pp. 1-34, June. 2020.
- [22] A. Krizhevsky *et al.*, "ImageNet Classification with Deep Convolutional Neural Networks," in *Proc. Adv. Neural Inf. Process. Syst.*, 2012, pp.1097-1105.
- [23] J. Redmon, S. Divvala, R. Girshick and A. Farhadi, "You Only Look Once: Unified, Real-Time Object Detection," in *Proc. IEEE Conf. Comput. Vision Pattern Recognit.*, 2016, pp. 779-788.
- [24] J. Redmon and A. Farhadi, "YOLO9000: Better, Faster, Stronger," in *Proc. IEEE Conf. Comput. Vision Pattern Recognit.*, 2017, pp. 6517-6525.
- [25] W. Liu *et al.*, "Ssd: Single shot multibox detector," in *Proc. Eur. Conf. Comput. Vision*, 2016, pp. 21-37.
- [26] R. Girshick, J. Donahue, T. Darrell and J. Malik, "Rich Feature Hierarchies for Accurate Object Detection and Semantic Segmentation," in *Proc. IEEE Conf. Comput. Vision Pattern Recognit.*, 2014, pp. 580-587.
- [27] R. Girshick, "Fast R-CNN," in *Proc. IEEE Int. Conf. Comput. Vision.*, 2015, pp. 1440-1448.
- [28] S. Ren, K. He, R. Girshick, and J. Sun, "Faster R-CNN: Towards Real-Time Object Detection with Region Proposal Networks," in *Proc. Adv. Neural Inf. Process. Syst.*, 2015, pp. 91-99.
- [29] K. He, G. Gkioxari, P. Dollár and R. Girshick, "Mask R-CNN," in *Proc. IEEE Int. Conf. Comput. Vision.*, 2017, pp. 2980-2988.
- [30] L. Karlinsky *et al.*, "RepMet: Representative-Based Metric Learning for Classification and Few-Shot Object Detection," in *Proc. IEEE Conf. Comput. Vision Pattern Recognit.*, 2019, pp. 5192-5201.
- [31] H. Chen *et al.*, "LSTD: A low-shot transfer detector for object detection," in *Proc. 32th AAAI Conf. Artif. Intell.*, 2018, pp. 2836-2843.
- [32] Y. Wang, D. Ramanan and M. Hebert, "Meta-Learning to Detect Rare Objects," in *Proc. IEEE Int. Conf. Comput. Vision.*, 2019, pp. 9924-9933.
- [33] X. Wang, T. Huang, J. Gonzalez, T. Darrell, and F. Yu, "Frustratingly Simple Few-Shot Object Detection," in *Proc. Int. Conf. Mach. Learn.*, 2020, pp. 9919-9928.
- [34] Q. Fan, W. Zhuo, C. -K. Tang and Y. -W. Tai, "Few-Shot Object Detection With Attention-RPN and Multi-Relation Detector," in *Proc. IEEE Conf. Comput. Vision Pattern Recognit.*, 2020, pp. 4012-4021.
- [35] R. Hadsell, S. Chopra and Y. LeCun, "Dimensionality Reduction by Learning an Invariant Mapping," in *Proc. IEEE Conf. Comput. Vision Pattern Recognit.*, 2006, pp. 1735-1742.
- [36] F. Schroff, D. Kalenichenko and J. Philbin, "FaceNet: A unified embedding for face recognition and clustering," in *Proc. IEEE Conf. Comput. Vision Pattern Recognit.*, 2015, pp. 815-823.
- [37] A. Mishchuk, D. Mishkin, F. Radenovic, and J. Matas, "Working Hard to Know Your Neighbor's Margins: Local Descriptor Learning Loss," in *Proc. Adv. Neural Inf. Process. Syst.*, 2017, pp. 4826-4837.
- [38] B. Harwood *et al.*, "Smart Mining for Deep Metric Learning," in *Proc. IEEE Int. Conf. Comput. Vision.*, 2017, pp. 2840-2848.
- [39] Y. Movshovitz-Attias, A. Toshev, T. K. Leung, S. Ioffe and S. Singh, "No Fuss Distance Metric Learning Using Proxies," in *Proc. IEEE Int. Conf. Comput. Vision.*, 2017, pp. 360-368.
- [40] Q. Qian *et al.*, "SoftTriple Loss: Deep Metric Learning Without Triplet Sampling," in *Proc. IEEE Int. Conf. Comput. Vision.*, 2019, pp. 6449-6457.
- [41] I. Elezi, S. Vascon, A. Torcinovich, M. Pelillo, L. Leal-Taixé, "The group loss for deep metric learning," in *Proc. Eur. Conf. Comput. Vision.*, 2020, pp. 277-294.
- [42] T. N. Kipf, and M. Welling, "Semi-Supervised Classification with Graph Convolutional Networks," in *Proc. Int. Conf. Learn. Representation.*, 2017.
- [43] P. Velickovic, G. Cucurull, A. Casanova, A. Romero, P. Liò, and Y. Bengio, "Graph Attention Networks," in *Proc. Int. Conf. Learn. Representation.*, 2018.
- [44] M. Chen, Z. Wei, Z. Huang, B. Ding, and Y. Li, "Simple and Deep Graph Convolutional Networks," in *Proc. Int. Conf. Mach. Learn.*, 2020, pp. 1725-1735.
- [45] X. Wang, Y. Ye and A. Gupta, "Zero-Shot Recognition via Semantic Embeddings and Knowledge Graphs," in *Proc. IEEE Conf. Comput. Vision Pattern Recognit.*, 2018, pp. 6857-6866.
- [46] M. Kampffmeyer, Y. Chen, X. Liang, H. Wang, Y. Zhang and E. P. Xing, "Rethinking Knowledge Graph Propagation for Zero-Shot Learning," in *Proc. IEEE Conf. Comput. Vision Pattern Recognit.*, 2019, pp. 11479-11488.
- [47] C. Lee, W. Fang, C. Yeh and Y. F. Wang, "Multi-label Zero-Shot Learning with Structured Knowledge Graphs," in *Proc. IEEE Conf. Comput. Vision Pattern Recognit.*, 2018, pp. 1576-1585.
- [48] L. Liu *et al.*, "Attribute Propagation Network for Graph Zero-shot Learning," in *Proc. 34th AAAI Conf. Artif. Intell.*, 2020, pp. 4868-4875.
- [49] C. Yan, Q. Zheng, X. Chang, M. Luo, C. -H. Yeh and A. G. Hauptman, "Semantics-Preserving Graph Propagation for Zero-Shot Object Detection," *IEEE Trans. Image. Processing.*, vol. 29, pp. 8163-8176, July. 2020.
- [50] H. Hu *et al.*, "Class-wise dynamic graph convolution for semantic segmentation," in *Proc. Eur. Conf. Comput. Vision*, 2020, pp. 1-17.
- [51] M. Everingham, L. Gool, C. K. Williams, J. Winn, and A. Zisserman, "The Pascal Visual Object Classes (VOC) Challenge," in *Int. Journal. Comput. Vision.*, 2010, pp. 303-338.
- [52] T. -Y. Lin *et al.*, "Microsoft COCO: Common Objects in Context," in *Proc. Eur. Conf. Comput. Vision.*, 2014, pp. 740-755.
- [53] L. Maaten and G. Hinton, "Visualizing non-metric similarities in multiple maps," in *Machine Learning.*, vol. 87, pp. 33-55, April. 2012.